Drop-on-Demand Inkjet Printhead Performance Improvement Using Robust Feedforward Control

Amol A. Khalate, Benoît Bayon, Xavier Bombois, Gérard Scorletti, Robert Babuška

Abstract— The printing quality delivered by a Drop-on-Demand (DoD) inkjet printhead is mainly limited due to the residual oscillations in the ink channel. The maximal jetting frequency of a DoD inkjet printhead can be increased by quickly damping the residual oscillations and by bringing in this way the ink-channel to rest after jetting the ink drop. The inkjet channel model obtained is generally subjected to parametric uncertainty. This paper proposes a robust optimization-based method to design the input actuation waveform for the piezo actuator in order to improve the damping of the residual oscillations in the presence of parametric uncertainties in the ink-channel model. Simulation results are presented to show the efficacy of the proposed method.

I. INTRODUCTION

The ability of inkjet technology to deposit materials with diverse chemical and physical properties has made it an important technology for both industry and home use. Apart from conventional document printing, the inkjet technology has been successfully applied in the areas of electronics, mechanical engineering and life sciences [1]. This is mainly thanks to the low operational costs of the technology. Typically, a drop-on-demand (DoD) inkjet printhead consists of several ink channels in parallel. Each channel is provided with a piezo-actuator, which on application of a voltage pulse can generate pressure oscillations inside the ink channel. These pressure oscillations push the ink drop out of the nozzle [2]. The print quality delivered by an inkjet printhead depends on the properties of the jetted drop, i.e., the drop velocity, the jetting direction and the drop volume. To meet the challenging performance requirements posed by new applications, these drop properties have to be tightly controlled.

The performance of the inkjet printhead is mainly limited due to the *residual pressure oscillations*. The actuation pulses are designed to provide an ink drop of a specified volume and velocity under the assumption that the ink channel is in steady state. Once the ink drop is jetted, the pressure oscillations inside the ink channel take several micro-seconds to decay. If the next ink drop is jetted before the residual

pressure oscillations settle, the resulting drop properties will be different from the ones of the previous drop. Therefore, at a high jetting frequency (which is also called the DoD frequency), drops will be jetted before the oscillations in the ink channel have completely disappeared and these residual oscillations will influence the drop velocity. This can degrade the printhead performance, since a printhead has to jet drops with a constant velocity at different frequencies.

In the literature, we can find various methods [3], [4], [5], [6] to design the piezo actuation pulse. In [7] we have proposed an optimization-based method to design the actuation pulse using a discrete-time model $H(q)$ relating the piezo input voltage (i.e., the input u) to the velocity of the meniscus (i.e., the output y). The meniscus is an interface between the ink and air. We consider this particular model since it is well known that the velocity of the meniscus is a good measure of the pressure in the ink channel. Consequently, reducing the residual oscillations of the meniscus velocity is equivalent to reducing the residual pressure oscillations in the ink channel. In our latest work [8] we have shown that the dynamical model $H(q)$ from the piezo input to the meniscus velocity changes considerably while jetting at various operating DoD frequencies. A compact polytopic uncertainty $\Delta \in \mathbf{\Delta}$ on the coefficients of the nominal inkjet system is presented such that the uncertain model $H(q, \Delta)$, encompasses the set of dynamics at various operating DoD frequencies. The actuation pulse is parameterized as a pulse response of a to-be-designed filter $F(q)$. Thus, the robust pulse is determined as the one minimizing the worst-case H_2 norm of the tracking error given as follows

$$\mathcal{J}(F) = \max_{\Delta \in \mathbf{\Delta}} \left\| H_{\text{ref}}(q) - H(q, \Delta)F(q) \right\|_2^2. \tag{1}$$

where the pulse response of $H_{\text{ref}}(q)$ is the reference meniscus velocity trajectory $y_{\text{ref}}(k)$ (i.e., a meniscus velocity profile with fast decaying residual oscillations). The experimental results show that the robust pulse designed with the proposed approach in [8] improve the printhead performance substantially.

The robust pulse design proposed in [8] use a FIR model structure for a to-be-designed filter $F(q, \beta)$ with β the filter coefficient vector. Thus, the dimension of the filter coefficient vector β is equal to the number of samples in the actuation pulse $u(k)$. The dimension of the to-be-designed β will become larger when the actuation pulse is longer and/or when the sampling time T_s is shorter. This may pose numerical problems since the size of the LMI problem, required to obtain the robust filter $F(q, \beta)$,

Amol A. Khalate, Xavier Bombois, Robert Babuška are with the Delft Center for Systems and Control, Delft University of Technology, Mekelweg 2, 2628 CD, Delft, The Netherlands, email: {a.a.khalate, x.j.a.bombois, r.babuska}@tudelft.nl.

Benoît Bayon and Gérard Scorletti are with Laboratoire Ampére, Ecole Centrale de Lyon, 36 avenue Guy de Collongue - 69134 Ecully Cedex, France. email: {Benoit.Bayon, Gerard.Scorletti}@ec-lyon.fr.

is directly proportional to the dimension of vector β. One can tackle this problem by choosing an appropriate set of orthogonal basis functions (OBFs) and weighting them in order to reduce the performance index (1). However, a more general approach is to let $F(q)$ be a rational function.

In the literature, the problem of designing a robust H_2 filter is considered by many authors. Since, a class of feedforward control problems turns out to be dual to the filtering problem, we can utilize these classical results to design the robust actuation pulse. We are dealing with a discrete-time system with a polytopic uncertainty. For this type of uncertainty we can extend the results of [9] to design the robust H_2 feedforward control. One of the drawback of this design method is that it uses a constant Lyapunov function at the vertices of the polytope, which may introduce conservatism. In this paper, we propose new conditions to design the robust filter $F(q)$ by introducing parameter-dependent Lyapunov functions, which improve the results in many cases. We provide simulation results for the inkjet system to show the performance improvement using the proposed method.

II. System description and modeling

Consider the discrete-time model $H(q)$, similar to [8][1], which describes the dynamics from the piezo input voltage u to the meniscus velocity y is given as follows

$$H(q) = g \left(\frac{q^2 + b_1 q + b_2}{q^2 + a_1 q + a_2} \right) \left(\frac{q + b_3}{q^2 + a_3 q + a_4} \right) \qquad (2)$$

where q is the forward shift operator and the nominal values of the coefficients are

$$b_1 = -3.4465, b_2 = 2.4575, b_3 = -5.7462 \times 10^{-1},$$
$$a_1 = -1.9538, a_2 = 9.6960 \times 10^{-1}, a_3 = -1.9102,$$
$$a_4 = 9.7322 \times 10^{-1}, g = 1.1820 \times 10^{-3}.$$

The sampling time T_s is chosen equal to 0.25μs. This inkjet system can be represented in the state-space form as follows

$$x_S(k+1) = A_S x_S(k) + B_S u(k)$$
$$y(k) = C_S x_S(k) \qquad (3)$$

where

$$A_S = \begin{bmatrix} 0 & -a_2 & 0 & 0 \\ 1 & -a_1 & 0 & 0 \\ 0 & b_3 & 0 & -a_4 \\ 0 & 1 & 1 & -a_3 \end{bmatrix}, B_S = \begin{bmatrix} g(b_2 - a_2) \\ g(b_1 - a_1) \\ gb_3 \\ g \end{bmatrix},$$
$$C_S = \begin{bmatrix} 0 & 0 & 0 & 1 \end{bmatrix}. \qquad (4)$$

As discussed in [8], at different DoD frequencies, the dynamics from the piezo input to the meniscus velocity $H(q)$ will not be the same. It is observed that the first resonant mode of the inkjet system varies a lot compared to the second resonant mode. It is possible to represent these multiple models obtained at different operating DoD frequencies by

[1] The difference is that [8] uses a proper transfer function and that the transfer function considered in this paper is strictly proper. It does not change the frequency response in the dominant low frequency range. However, having a strictly proper function will simplify the pulse design.

the nominal plant (2) with uncertainty on its coefficients. An uncertainty Δ on the coefficients a_1 and a_2 of (2) is chosen such that the uncertain system $H(q, \Delta)$ encompasses the set of models obtained at different operating DoD frequencies. The uncertainty $\Delta = [\Delta^{(1)} \quad \Delta^{(2)}]^T$ perturbs the coefficients a_1 and a_2 in the following manner:

$$a_1(\Delta) = a_{1,\text{nom}}(1 + \Delta^{(1)}) \qquad (5)$$
$$a_2(\Delta) = a_{2,\text{nom}}(1 + \Delta^{(2)}), \qquad (6)$$

where $a_{1,\text{nom}} = -1.954$ and $a_{2,\text{nom}} = 0.9696$ are the nominal values of the coefficients a_1 and a_2. The uncertainty Δ on the coefficients lie inside the polytope $\boldsymbol{\Delta}$ which is formed by convex combination of the four vertices Δ_i, $i = 1, 2, 3, 4$, i.e. $\Delta \in \boldsymbol{\Delta} = \text{conv}(\Delta_1, \Delta_2, \Delta_3, \Delta_4)$. The values of these four vertices computed via system identification results (for details see [8]) are $\Delta_1 = [0.8103/100 \quad 1.3928/100]^T$, $\Delta_2 = [0.4031/100 \quad 1.0927/100]^T$, $\Delta_3 = [-0.0342/100 \quad -0.3206/100]^T$, $\Delta_4 = [-0.5813/100 \quad -0.9097/100]^T$.

It can be seen that the uncertainty Δ enters affinely in the matrices A_S and B_S (3). Thus, the state-space matrices of the inkjet system $H(q, \Delta)$ for the admissible uncertainty $\Delta \in \boldsymbol{\Delta}$ belong to the polytope

$$\left[A_S(\Delta), B_S(\Delta) \right] = \sum_{i=1}^{4} \alpha_i \left[A_{S_i}, B_{S_i} \right], \qquad (7)$$

where the matrices $A_{S_i} = A_S(\Delta_i)$, $B_{S_i} = B_S(\Delta_i)$, $i = 1, ..., 4$, are the system matrices of a fixed inkjet system at the i-th vertex of the polytope and α_i are positive scalars such that $\sum_{i=1}^{4} \alpha_i = 1$. The matrix C_S is independent of Δ. In the next section, we use this uncertain model of the inkjet system $H(q, \Delta)$ in order to design a robust actuation pulse.

III. Robust feedforward control

Generally, commercial inkjet printheads use actuation pulses with shape constraints (for details, see [7]) which are mainly due to electronic hardware limitations. However, for future high-end inkjet printheads this shape constraint on the actuation pulse may restrict the printhead performance. Rapid developments in the electronics field will enable printhead manufacturers to use more sophisticated electronic hardware which can generate an unconstrained actuation pulse. Therefore, it is essential to investigate the possibility of an unconstrained actuation pulse which will damp the residual oscillations when the inkjet channel model is subjected to parametric uncertainty. In this section, we first review the robust actuation pulse design using the H_2 feedforward formulation presented in [8]. Further, we provide an extension of [9] to design a robust pulse using a constant Lyapunov function and finally, we give improved conditions using parameter-dependent Lyapunov functions.

A. Robust actuation pulse using H_2 feedforward control

In [7], we have designed a meniscus velocity profile $y_{\text{ref}}(k)$ with fast decaying residual oscillations. As shown in Fig. 1, the reference trajectory $y_{\text{ref}}(k)$ is modeled as the pulse response of a rational function $H_{\text{ref}}(q)$. The state-space
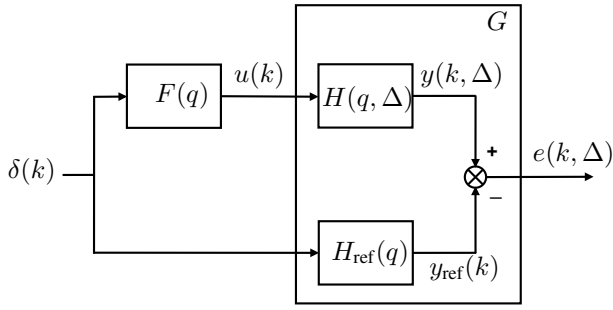
Fig. 1. Filtering problem for the inkjet printhead.

representation of the reference model $H_{\text{ref}}(q)$ is given as follows

$$x_R(k+1) = A_R x_R(k) + B_R \delta(k)$$
$$y_{\text{ref}}(k) = C_R x_R(k) \qquad (8)$$

where $\delta(k)$ is the unit pulse. If the actuation pulse $u(k)$ is designed in such a way that the meniscus velocity $y(k)$ follows the reference trajectory $y_{\text{ref}}(k)$, then the channel will come to rest very quickly after jetting the ink drop. This will create a condition to jet the ink drops at higher jetting frequencies.

In the previous section, we have presented a compact polytopic uncertainty $\Delta \in \mathbf{\Delta}$ on the coefficients of the inkjet system such that uncertain system $H(q, \Delta)$ represents the set of multiple models obtained at various operating DoD frequencies. The state-space representation of the system $G(q)$ (see Fig. 1) with two inputs and the tracking error e as the output is given as follows:

$$\left[\begin{array}{c|cc} \tilde{A}(\Delta) & \tilde{B}_S(\Delta) & \tilde{B}_R \\ \hline \tilde{C} & 0 & 0 \end{array} \right] = \left[\begin{array}{cc|cc} A_S(\Delta) & 0 & B_S(\Delta) & 0 \\ 0 & A_R & 0 & B_R \\ \hline C_S & -C_R & 0 & 0 \end{array} \right].$$

The uncertainty in the inkjet channel model can now be handled owing to the H_2 filtering formulation. For this purpose, we parameterize the actuation pulse as the pulse response of a filter $F(q)$:

$$u(k) = F(q)\delta(k) \qquad (9)$$

where $\delta(k)$ the unit pulse and the state-space representation of the filter $F(q)$ is given as follows

$$x_F(k+1) = A_F x_F(k) + B_F \delta(k)$$
$$u(k) = C_F x_F(k) + D_F \delta(k). \qquad (10)$$

The state-space representation of the uncertain error dynamics (from the input $\delta(k)$ to the tracking error $e(k, \Delta)$), $\nu(q, F, \Delta) = \left(H_{\text{ref}}(q) - H(q, \Delta)F(q) \right)$ is given as follows:

$$\left[\begin{array}{c|c} A(\Delta) & B(\Delta) \\ \hline C & 0 \end{array} \right] = \left[\begin{array}{cc|c} A_F & 0 & B_F \\ \tilde{B}_s(\Delta)C_F & \tilde{A}(\Delta) & \tilde{B}_s(\Delta)D_F + \tilde{B}_R \\ \hline 0 & \tilde{C} & 0 \end{array} \right]$$
$$(11)$$

In the sequel, we impose the dimension of A_F to be equal to the one of $\tilde{A}(\Delta)$. It is indeed shown in [10] that the optimal filter has this dimension. As we assume the uncertainty Δ to

be of a polytopic nature ($\Delta \in \mathbf{\Delta}$), the state-space matrices of the error system $\nu(q, F, \Delta)$ belong to the following polytope

$$\left[A(\Delta), B(\Delta) \right] = \sum_{i=1}^{4} \alpha_i \left[A_i, B_i \right], \qquad (12)$$

where the matrices $\left(A_i, B_i \right)$ are the state-space matrices of the fixed error dynamics $\nu_i(q, F)$ at the i-th vertex of the polytope and α_i are positive scalars such that $\sum_{i=1}^{4} \alpha_i = 1$. The matrix C is independent of Δ. Clearly, the uncertain system error dynamics is a convex combination of the fixed systems at the vertices of the polytope $\mathbf{\Delta}$.

For a nominal system, the performance of the filter $F(q)$ can be defined as the H_2 norm of the tracking error. Here, we have an uncertain inkjet system $H(q, \Delta)$ which is perturbed by the uncertainty $\Delta \in \mathbf{\Delta}$. Therefore, we must obtain a robust actuation pulse whose performance is good over the polytopic uncertainty, rather than obtaining an optimal actuation pulse whose performance is only good for the nominal inkjet system. Thus, it is a good choice to define the performance index $\mathcal{J}(\beta)$ as the square of the worst-case H_2 norm of the tracking error transfer function $\nu(q, \beta, \Delta)$:

$$\mathcal{J}(F) = \max_{\Delta \in \mathbf{\Delta}} \left\| \nu(q, F, \Delta) \right\|_2^2 = \max_{\Delta \in \mathbf{\Delta}} \left\| H_{\text{ref}}(q) - H(q, \Delta)F(q) \right\|_2^2.$$
$$(13)$$

The robust filter F_{robust}, describing the unconstrained robust actuation pulse is, thus, the solution F_{robust} of the following optimization problem

$$[\gamma_{\text{opt}}, F_{\text{robust}}] = \arg \min_{\gamma, F} \gamma, \quad \text{subject to} \quad \mathcal{J}(F) < \gamma, \quad (14)$$

where the solution γ_{opt} is the minimal worst-case H_2 norm that can be achieved by a filter $F(q)$ (see Fig. 1) and F_{robust} is the filter achieving this minimal worst-case H_2 norm.

It is difficult to obtain the solution of the above problem as it is not a convex finite dimensional optimization problem. However, it is possible to compute an upper bound on γ_{opt} and a suboptimal filter using convex optimization. In [8], the upper bound on γ_{opt} is obtained using LMIs conditions with a filter $F(q, \beta)$ restricted to an FIR model structure with β the filter coefficient vector. As explained in the introduction, the dimension of the to-be-designed vector β will become larger when the actuation pulse is longer and/or when the sampling time T_s is smaller. This may pose numerical problems since the size of the LMI problem, required to obtain the robust filter $F(q, \beta)$, is directly proportional to the dimension of vector β. A general approach to overcome this problem is to chose $F(q)$ as a rational function.

The results for the design of the robust filter F_{robust} are based on the results for the design of a filter F_{opt} for the nominal plant $H(q)$ in (2) (i.e. the plant $H(q, \Delta)$ with $\Delta = [0 \ 0]^T$). For simplicity, we first present a methodology to design this nominal filter F_{opt} i.e. the filter solving the following problem

$$[\gamma_{\text{opt}}^{\text{nom}}, F_{\text{opt}}] = \arg \min_{\gamma^{\text{nom}}, F} \gamma^{\text{nom}},$$
$$\text{subject to} \quad \mathcal{J}_{\text{nom}}(F) < \gamma^{\text{nom}}, \qquad (15)$$

with $\mathcal{J}_{\text{nom}}(F) = \left\| H_{\text{ref}}(q) - H(q)F(q) \right\|_2^2$.

We will see in the following lemma, as opposed to the robust case, the solution of the problem (15) can be computed exactly.

Note that we use $*$ as an ellipsis for terms that can be induced by symmetry.

Lemma 1: Consider the optimization problem (15). The solution $\gamma_{\text{opt}}^{\text{nom}}$ of (15) can be exactly computed as the solution of the following LMI optimization problem

$$\min_{\gamma^{\text{nom}},W=W^T,Q=Q^T,Z=Z^T,\tilde{A}_F,B_F,\tilde{C}_F,D_F} \gamma^{\text{nom}}$$

such that $\quad \text{trace}[W] < \gamma^{\text{nom}}$

$$\begin{bmatrix} P & S_1 & S_2 \\ * & P & 0 \\ * & * & I \end{bmatrix} > 0, \quad \begin{bmatrix} W & S_3 \\ * & P \end{bmatrix} > 0 \quad (16)$$

where $P = \begin{bmatrix} (Q-Z) & (Q-Z) \\ * & Q \end{bmatrix}, S_2 = \begin{bmatrix} B_F \\ \tilde{B}_S D_F + \tilde{B}_R \end{bmatrix}$

$$S_1 = \begin{bmatrix} \tilde{A}_F & \tilde{A}_F \\ \tilde{B}_S\tilde{C}_F + \tilde{A}(Q-Z) & \tilde{B}_S\tilde{C}_F + \tilde{A}Q \end{bmatrix} \quad (17)$$

$$S_3 = \begin{bmatrix} \tilde{C}(Q-Z) & \tilde{C}Q \end{bmatrix}.$$

The state-space matrices in the above LMIs corresponds to the state-space matrices (11) of $\nu(q, F, \Delta)$ with $\Delta = [0\ \ 0]^T$, i.e. the error dynamics with the nominal system $H(q)$.

The optimal filter $F_{\text{opt}}(q)$ achieving $\mathcal{J}_{\text{nom}}(F) = \gamma_{\text{opt}}^{\text{nom}}$ can then be computed as follows using the decision variables Q_{opt}, Z_{opt}, $\tilde{A}_{F_{\text{opt}}}$, $B_{F_{\text{opt}}}$, $\tilde{C}_{F_{\text{opt}}}$ and $D_{F_{\text{opt}}}$ solving the above LMI problem

$$F_{\text{opt}} = \left[\begin{array}{c|c} A_{F_{\text{opt}}} & B_{F_{\text{opt}}} \\ \hline C_{F_{\text{opt}}} & D_{F_{\text{opt}}} \end{array} \right] = \left[\begin{array}{c|c} \tilde{A}_{F_{\text{opt}}}(Q_{\text{opt}} - Z_{\text{opt}})^{-1} & B_{F_{\text{opt}}} \\ \hline \tilde{C}_F(Q_{\text{opt}} - Z_{\text{opt}})^{-1} & D_{F_{\text{opt}}} \end{array} \right].$$

Proof: Consider the error dynamics system (11) (i.e. the system G augmented with the filter F) without the uncertainty Δ and for one particular $F(q)$. Then, it is well known [9] that for $\gamma^{\text{nom}} > 0$ the inequality $\|\nu(q)\|_2^2 < \gamma^{\text{nom}}$ holds if and only if there exist symmetric matrices P and W such that

$$\text{trace}[W] < \gamma^{\text{nom}}, \quad \begin{bmatrix} P & AP & B \\ * & P & 0 \\ * & * & I \end{bmatrix} > 0, \quad \begin{bmatrix} W & CP \\ * & P \end{bmatrix} > 0,$$
$$(18)$$

where the matrices A, B, C correspond to the state-space matrices (11) of $\nu(q, F, \Delta)$ with $\Delta = [0\ \ 0]^T$, i.e. the error dynamics with the nominal system $H(q)$. By using the partition of the Lyapunov function P given in (17) and by using the following change of variables $\tilde{A}_F = A_F(Q - Z)$ and $\tilde{C}_F = C_F(Q - Z)$ we can rewrite (18) as (16). The expression of the optimal filter F_{opt} follows then directly from the definition of $\tilde{A}_F$ and $\tilde{C}_F$. ∎

Remark: Lemma 1 is close to the result in [9]. However, we use here another partition of P (see (17)) which simplifies the derivation of the filter.

B. Robust actuation pulse design using a rational filter

We have seen that Lemma 1 can be used to design an optimal pulse using a rational filter $F(q)$. By extending these results, an upper bound $\gamma_{\text{opt}}^{\text{UB}}$ on the solution γ_{opt} of the problem (14) can be obtained using the following theorem.

Theorem 1: Consider the error dynamics given by (11) with the polytopic uncertainty (12) then, $\gamma_{\text{opt}}^{\text{UB}}$, the solution of the following LMI optimization problem, is guaranteed to be an upper bound of the solution γ_{opt} of the problem (14)

$$\min_{\gamma^{\text{UB}},W=W^T,Q=Q^T,Z=Z^T,\tilde{A}_F,B_F,\tilde{C}_F,D_F} \gamma^{\text{UB}}$$

such that following LMIs hold for $i = 1, 2, 3, 4$

$$\text{trace}[W] < \gamma^{\text{UB}}$$

$$\begin{bmatrix} P & S_1(\Delta_i) & S_2(\Delta_i) \\ * & P & 0 \\ * & * & I \end{bmatrix} > 0, \quad \begin{bmatrix} W & S_3 \\ * & P \end{bmatrix} > 0 \quad (19)$$

where

$$P = \begin{bmatrix} (Q-Z) & (Q-Z) \\ * & Q \end{bmatrix}, S_2(\Delta_i) = \begin{bmatrix} B_F \\ \tilde{B}_S(\Delta_i) D_F + \tilde{B}_R \end{bmatrix}$$
$$S_1(\Delta_i) = \begin{bmatrix} \tilde{A}_F & \tilde{A}_F \\ \tilde{B}_S(\Delta_i)\tilde{C}_F + \tilde{A}(\Delta_i)(Q-Z) & \tilde{B}_S(\Delta_i)\tilde{C}_F + \tilde{A}(\Delta_i)Q \end{bmatrix}$$
$$S_3 = \begin{bmatrix} \tilde{C}(Q-Z) & \tilde{C}Q \end{bmatrix}, \quad (20)$$

and the robust filter $F_{\text{robust}}(q)$ which is guaranteed to achieve (at most) a worst-case norm of $\gamma_{\text{opt}}^{\text{UB}}$ is

$$F_{\text{robust}} = \left[\begin{array}{c|c} A_F & B_F \\ \hline C_F & D_F \end{array} \right] = \left[\begin{array}{c|c} \tilde{A}_F(Q-Z)^{-1} & B_F \\ \hline \tilde{C}_F(Q-Z)^{-1} & D_F \end{array} \right].$$

Proof: The LMI (19) for a given i is equivalent to the LMI (16) for the error dynamics system $\nu(q, F, \Delta_i)$. Verifying that the LMI (19) holds for $i = 1, 2, 3, 4$, is thus equivalent to verify that $\|\nu(q, F, \Delta_i)\|_2^2 < \gamma^{\text{UB}}$ for the systems $\nu(q, F, \Delta_i)$ at the vertices of the polytopic uncertainty $\boldsymbol{\Delta}$. Since the uncertainty Δ enters linearly in the LMI's ($S_1(\Delta)$ and $S_2(\Delta)$ are indeed affine in Δ), the above fact implies that $\|\nu(q, F, \Delta)\|_2^2 < \gamma^{\text{UB}}$ for all $\Delta \in \boldsymbol{\Delta}$ (see e.g. [11]). The construction of the filter is then similar as in Lemma 1. ∎

Remark: We observe that the LMI conditions (19) proposed to obtain the robust filter F_{robust} should be valid at all vertices $\Delta_i, i = 1, ..., 4$ of the polytope $\boldsymbol{\Delta}$ with a constant Lyapunov function P. This stringent restriction may lead to conservative results, i.e. $\gamma_{\text{opt}}^{\text{UB}} >> \gamma_{\text{opt}}$. If we allow the Lyapunov function P to be parameter dependent, i.e. $P(\Delta)$, the condition (19) will no longer be an LMI because the Lyapunov function P and the state-space variables of the filter $F(q)$ are closely interconnected. Similar to [10], to overcome this difficulty we will utilize a reciprocal variant of the projection lemma to alleviate the interrelation between P and the filter variables. This result is presented in Theorem 2.

Theorem 2: Consider the error dynamics given by (11) with the polytopic uncertainty (12). If the following LMI optimization problem is feasible

$$\min_{\gamma^{\text{UB}},W=W^T,P=P^T,Z,L} \gamma^{\text{UB}}$$

such that following LMIs hold for $i = 1, 2, 3, 4$

$$\text{trace}[W] < \gamma^{\text{UB}}$$

$$\begin{bmatrix} P(\Delta_i) & * & * \\ S_4(\Delta_i) & S_5 - P(\Delta_i) & * \\ S_6(\Delta_i) & S_7 & L_{33} + L_{33}^T - I \end{bmatrix} > 0, \quad (21)$$

$$\begin{bmatrix} W & * \\ S_8(\Delta_i) & P(\Delta_i) \end{bmatrix} > 0 \quad (22)$$

where

$$P(\Delta_i) = \begin{bmatrix} P_1(\Delta_i) & * \\ P_3(\Delta_i) & P_2(\Delta_i) \end{bmatrix}, L = \begin{bmatrix} L_{11} & L_{12} & L_{13} \\ L_{11} & L_{22} & L_{13} \\ L_{31} & L_{32} & L_{33} \end{bmatrix}$$

$$S_4(\Delta_i) = \begin{bmatrix} -Z_{11}^T & -(Z_{21}^T \tilde{B}_S(\Delta_i)^T + L_{12}A(\Delta_i)^T + L_{13}\tilde{B}_R^T) \\ -Z_{11}^T & -(Z_{21}^T \tilde{B}_S(\Delta_i)^T + L_{22}A(\Delta_i)^T + L_{13}\tilde{B}_R^T) \end{bmatrix}$$

$$S_6(\Delta_i) = \begin{bmatrix} -Z_{12}^T & -(Z_{22}^T \tilde{B}_S(\Delta_i)^T + L_{32}A(\Delta_i)^T + L_{33}\tilde{B}_R^T) \end{bmatrix}$$

$$S_8(\Delta_i) = \begin{bmatrix} \tilde{C}P_3(\Delta_i) & \tilde{C}P_2(\Delta_i) \end{bmatrix}^T$$

$$S_5 = \begin{bmatrix} L_{11} + L_{11}^T & * \\ L_{11} + L_{12}^T & L_{22} + L_{22}^T \end{bmatrix}, Z = \begin{bmatrix} Z_{11} & Z_{12} \\ Z_{21} & Z_{22} \end{bmatrix}$$

$$S_7 = \begin{bmatrix} L_{31} + L_{13}^T & L_{32} + L_{13}^T \end{bmatrix}, \quad (23)$$

then $\gamma_{\text{opt}}^{\text{UB}}$, the solution of the above LMI optimization problem is guaranteed to be an upper bound on the solution γ_{opt} of the problem(14). Moreover, the robust filter $F_{\text{robust}}(q)$ which is guaranteed to achieve (at most) a worst-case norm of $\gamma_{\text{opt}}^{\text{UB}}$ is

$$F = \left[\begin{array}{c|c} A_F & B_F \\ \hline C_F & D_F \end{array}\right] = \begin{bmatrix} L_{11}^T & L_{31}^T \\ L_{13}^T & L_{33}^T \end{bmatrix}^{-1} \begin{bmatrix} Z_{11} & Z_{12} \\ Z_{21} & Z_{22} \end{bmatrix}. \quad (24)$$

Proof: Consider the error dynamics system (11) (i.e. the system G augmented with the filter F) for one particular Δ and for one particular $F(q)$, then the inequality $\|\nu(q, F, \Delta)\|_2^2 < \gamma^{\text{UB}}$ holds if and only if we can find γ^{UB} such that trace$[W] < \gamma^{\text{UB}}$ and the following inequalities hold

$$\begin{bmatrix} I & A(\Delta) & B(\Delta) \end{bmatrix} \Psi(\Delta)[*]^T > 0, \quad (25)$$

$$\begin{bmatrix} W & * \\ S_8(\Delta) & P(\Delta) \end{bmatrix} > 0 \quad (26)$$

where $\Psi(\Delta) = \text{diag}(P(\Delta), -P(\Delta), -I)$. The above conditions are equivalent with those in (18). We use the notation $P(\Delta)$ because the Lyapunov matrices P can be different for different values of Δ. Note that the condition (26) is an LMI, but the condition (25) is not.

In order to obtain a convex robust optimization problem, we need to rewrite (25) as a matrix inequality where $P(\Delta)$ does not multiply with any Δ-dependent term. The condition (25) can be rewritten using the projection lemma (see Appendix A.1). This projection lemma state that (25) holds if and only if there exists a matrix $L(\Delta)$ of appropriate dimension satisfying the following inequality

$$\Psi(\Delta) + U(\Delta)^T L^T(\Delta) V + V^T L(\Delta) U(\Delta) > 0 \quad (27)$$

with $V = \begin{bmatrix} 0 & I & 0 \\ 0 & 0 & I \end{bmatrix}, U(\Delta) = \begin{bmatrix} -A^T(\Delta) & I & 0 \\ -B^T(\Delta) & 0 & I \end{bmatrix}$,

Note that $L(\Delta)$ in (27) is also function of Δ. However, in sequel we will consider a constant L in order to obtain an LMI formulation. In (27), L has no special structure. However, in Theorem 2, we impose the special structure on L given by (23). If we can find a matrix having

this structure, then (25) holds. Otherwise, we cannot say anything about (25).

Supposing first that a matrix L exists, with $S_4(\Delta), S_5, S_6(\Delta), S_7$ as defined in (23) and with the following change of variables

$$\begin{bmatrix} Z_{11} & Z_{12} \\ Z_{21} & Z_{22} \end{bmatrix} = \begin{bmatrix} A_F & B_F \\ C_F & D_F \end{bmatrix} \begin{bmatrix} L_{11}^T & L_{31}^T \\ L_{13}^T & L_{33}^T \end{bmatrix} \quad (28)$$

we can rewrite (27) as follows:

$$\begin{bmatrix} P(\Delta) & * & * \\ S_4(\Delta) & S_5 - P(\Delta) & * \\ S_6(\Delta) & S_7 & L_{33} + L_{33}^T - I \end{bmatrix} > 0. \quad (29)$$

In (29), we observe that $P(\Delta)$ does not multiply terms which are functions of Δ. Moreover, the uncertainty Δ appears linearly in $S_4(\Delta)$ and $S_7(\Delta)$. Finally, (29) is affine in the variables $P(\Delta)$, Z and L.

Summarizing, if there exists a matrix L having the special structure given in (23), such that trace$[W] < \gamma^{\text{UB}}$, (26) and (29) holds then $\|\nu(q, F, \Delta)\|_2^2 < \gamma^{\text{UB}}$ for a given Δ and F. Using the convex combination property [11], we can also say that if there exists L and Z such that trace$[W] < \gamma^{\text{UB}}$, (26) and (29) holds for $\Delta = \Delta_i$, $i = 1, 2, 3, 4$, then $\|\nu(q, F, \Delta)\|_2^2 < \gamma^{\text{UB}}$ for all $\Delta \in \boldsymbol{\Delta}$. Moreover, because of (28), the corresponding filter is given as in (23). ∎

Remark: We know that the solution of Theorem 1 is an upper bound on the solution γ_{opt} of the problem (14), but this does not hold for Theorem 2. If the new conditions in Theorem 2 with the parameter dependent Lyapunov functions are feasible then, indeed, it delivers an upper bound on the solution γ_{opt} of the problem (14). However, when the conditions in Theorem 2 are not feasible we cannot say anything about the upper bound. The reason for this is that it is not always possible to obtain L in (27) with the proposed special structure to ensure (25). Nevertheless, when the LMI problem (21)-(22) is feasible, in many cases, it will provide a less conservative result (see e.g. [10]).

In the next section, we present simulation results for the inkjet system with the robust actuation pulses designed with the above two theorems.

IV. SIMULATION RESULTS

Generally, in the printhead industry the actuation pulses are designed with the nominal model $H(q)$ (see [7]). It is possible to design an unconstrained optimal actuation pulse $u_{\text{opt}}(k)$ for the nominal model $H(q)$ using Lemma 1 (i.e., without considering the polytopic uncertainty). For this purpose, we use the desired meniscus velocity $y_{\text{ref}}(k)$ designed in [7], i.e., a template for the meniscus velocity with fast decaying residual oscillations. The black dash-dot line in Fig. 2 shows the unconstrained optimal pulse $u_{\text{opt}}(k) = F_{\text{opt}}(q)\delta(k)$ obtained after solving the optimization problem of Lemma 1 using the LMI Control Toolbox of MATLAB . The H_2 norm of the error dynamics $\nu(q, F_{\text{opt}})$ is found to be $\gamma_{\text{opt}}^{\text{nom}} = 0.1172$.
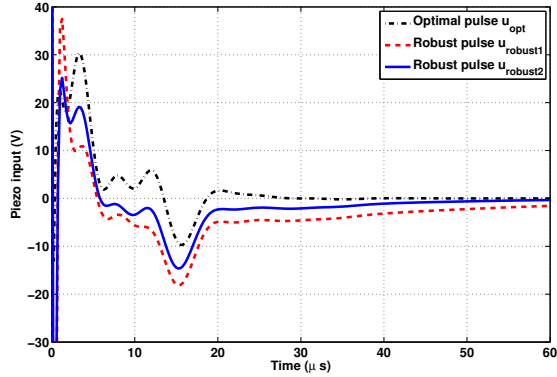
Fig. 2. Comparison of the actuation pulses obtained using Lemma 1, Theorem 1 and Theorem 2.

As discussed in the introduction, this optimal pulse may not perform satisfactorily in practice because the inkjet dynamics changes considerably while jetting at different DoD frequencies. Therefore, it is interesting to compute the worst-case H_2 norm of the error dynamics $\nu(q, F_{opt}, \Delta)$ for the polytopic uncertainty $\Delta \in \mathbf{\Delta}$ with the optimal filter $F_{opt}(q)$ to analyze the performance degradation. For the given filter $F_{opt}(q)$, we can compute a lower bound γ^{LB} on the worst-case H_2 norm by evaluating H_2 norm of $\nu(q, F_{opt}, \Delta)$ at fine grid points on the parametric uncertainty $\mathbf{\Delta}$. We found that the lower bound γ^{LB} on the worst-case H_2 norm with the optimal filter F_{opt} is 189.53.

We have solved the LMI optimization problem in Theorem 1 and Theorem 2 and the resulting robust pulses, $u_{robust1}(k)$ and $u_{robust2}(k)$ respectively are shown in Fig. 2. A numerical comparison of the worst-case H_2 norm of the error dynamics $\nu(q, \Delta)$ with these robust actuation pulses is presented in Table I. In Table I, we give also corresponding lower bound on γ_{opt} computed with a fine grid on the polytopic uncertainty $\mathbf{\Delta}$. Compared to the nominal filter F_{opt} achieving a worst-case norm of at least 189.53, the robust filters $F_{robust1}$ and $F_{robust2}$ achieve a much smaller worst-case norm. This is especially true with the pulse $u_{robust2}$ obtained with Theorem 2 (our improvement to Theorem 1). We also observe that the upper bound given by Theorem 2 is very close to the lower bound, which shows its efficacy for conservatism reduction.

TABLE I

COMPARISON OF THE WORST-CASE H_2 NORM OF THE ERROR DYNAMICS

$\nu(q, \Delta)$

	γ^{LB}	γ^{UB}_{opt}
Robust pulse $u_{robust1}(k)$ with Theorem 1	104.27	143.68
Robust pulse $u_{robust2}(k)$ with Theorem 2	52.21	70.82

V. CONCLUSION

In this paper, we have proposed a robust actuation pulse design method based on robust H_2 feedforward control to tackle the change in the inkjet system dynamics while

jetting at different DoD frequencies. We have relaxed the constraint of the FIR model structure on the to-be-designed robust filter presented in [8]. Further, we have provided improved conditions to compute the robust filter by allowing parameter dependent Lyapunov functions. Simulation results have demonstrated that a considerable improvement in the inkjet system performance can be achieved with the proposed robust robust pulses. Applications of the proposed method to multi-channel control and experimental testing will be investigated in the future. Even though the proposed robust feedforward control is demonstrated on the inkjet system it can be used for a wide range of industrial applications.

REFERENCES

[1] C. Williams, "Ink-jet printers go beyond paper," *Physics World*, vol. 19, pp. 24–29, 2006.
[2] M. Wassink, "Inkjet printhead performance enhancement by feedforward input design based on two-port modeling," Ph.D. dissertation, Delft University of Technology, 2007.
[3] D. Bogy and F. Talke, "Experimental and theoretical study of wave propagation phenomena in drop-on-demand ink jet devices," *IBM J. Res. Dev.*, vol. 28, no. 3, pp. 314–321, 1984.
[4] J. Chung, S. Ko, C. Grigoropoulos, N. Bieri, C. Dockendorf, and D. Poulikakos, "Damage-free low temperature pulsed laser printing of gold nanoinks on polymers," *Journal of Heat Transfer*, vol. 127, no. 7, pp. 724–732, Jul. 2005.
[5] K. Kwon and W. Kim, "A waveform design method for high-speed inkjet printing based on self-sensing measurement," *Sensors and Actuators A: Physical*, vol. 140, no. 1, pp. 75–83, 2007.
[6] K. Kwon, "Waveform design methods for piezo inkjet dispensers based on measured meniscus motion," *Journal of Microelectromechanical Systems*, vol. 18 (5), pp. 1118–1125, 2009.
[7] A. A. Khalate, X. Bombois, R. Babuška, H. Wijshoff, and R. Waarsing, "Optimization-based feedforward control for a drop-on-demand inkjet printhead," in *American Control Conference, Baltimore, MD, USA*, 2010.
[8] A. A. Khalate, X. Bombois, G. Scorletti, R. Babuška, R. Waarsing, and W. de Zeeuw, "Robust feedforward control for a drop-on-demand inkjet printhead," in *accepted for 18th IFAC World Congress*, 2011.
[9] J. Geromel, J. Bernussou, G. Garcia, and M. de Oliveira, "H_2 and H_∞ robust filtering for discrete-time linear systems," *SIAM J. Control Optim.*, vol. 38, pp. 1353–1368, 2000.
[10] H. Tuan, P. Apkarian, and T. Nguyen, "Robust and reduced-order filtering: new lmi-based characterizations and methods," *IEEE Transactions on Signal Processing*, vol. 49, no. 12, pp. 2975 –2984, Dec. 2001.
[11] S. Boyd, L. El Ghaoui, E. Feron, and V. Balakrishnan, *Linear Matrix Inequalities in System and Control Theory*, ser. Studies in Applied Mathematics. Philadelphia, PA: SIAM, Jun. 1994, vol. 15.

APPENDIX

A.1: Projection Lemma

Lemma:[10] Given a symmetric matrix $\Psi \in \mathbb{R}^{m \times m}$ and two matrices U, V of column dimension m, the following problem

$$\Psi + U^T L^T V + V^T L U > 0 \tag{30}$$

is solvable in a matrix L of compatible dimension if and only if

$$\mathcal{N}_U^T \Psi \mathcal{N}_U > 0, \quad \mathcal{N}_V^T \Psi \mathcal{N}_V > 0 \tag{31}$$

where $\mathcal{N}_U$ and $\mathcal{N}_V$ are any basis of the nullspace of U and V, respectively.